FREE-FALL OF SOLID PARTICLES THROUGH FLUIDS

Miloslav HARTMAN[a] and John G. YATES[b]

[a] *Institute of Chemical Process Fundamentals, Academy of Sciences of the Czech Republic, 165 02 Prague 6-Suchdol, The Czech Republic*

[b] *Department of Chemical and Biochemical Engineering, University College London, London WC1E7JE, England*

Received May 29, 1992
Accepted June 22, 1992

A comprehensive, up-to-date review is presented of predictive relationships for the terminal, free-fall velocity of solid particles falling in an infinite Newtonian fluid. The study explores accuracy of the implicit and explicit equations in terms of the drag coefficient and the terminal velocity. Problems of predicting the terminal velocity of non-spherical, isometric as well as non-isometric, particles are discussed.

1. INTRODUCTION

A situation, when there is the need to deal with the motion of particles in fluids, frequently occurs in chemical engineering problems. This phenomenon is of major importance in sedimentation, fluidization and in many other technological operations. The terminal or free-fall velocity of an isolated particle in an infinite fluid figures in most of the correlations for entrainment or elutriation of particles from the fluidized bed[1,2]. Such a quantity is also needed in gas and liquid cyclone design, crystallization and in other areas of chemical technology.

It has been, therefore, a frequent subject of investigation of mostly experimental studies. In the past decades, a considerable effort has been made to determine by experiment the terminal velocity and drag coefficient of freely falling spheres. Attempts at developing theoretical relationships betweeen the drag coefficient and the Reynolds number have been only partially successful. The application of such equations is limited to a region of low Reynolds numbers. In contrast to flow in a tube, both the resistance due to skin friction and that due to form drag effect flow around a sphere. The transition from the laminar to the turbulent region is not as well defined for flow around the sphere as it is for flow in a tube.

The present work has been undertaken with the objective of exploring the accuracy of the predictive expressions for the terminal velocity proposed in the literature. The comparison made also includes some of original work of the authors and their coworkers. At the same time it is hoped that this review provides a means for accurate and rapid prediction of the terminal velocity.

The findings given below on the terminal velocity apply in the absence of wall effects or concentration effects. In general, these effects are negligible for column-to-particle diameter ratios larger than about 100 and for volume concentrations lower than approximately 0.1%.

2. THEORETICAL

2. 1. *Physical Considerations*

The balance of forces acting on a spherical particle which is falling freely through an infinite fluid of constant density and viscosity is expressed as follows:

$$\text{Gravitational force} - \text{buoyancy force} - \text{drag force} = \text{acceleration force}. \qquad (1)$$

Such a situation is depicted in Fig. 1. The drag force can be written in terms of a drag coefficient C_D, the projected area perpendicular to the fluid flow A_p, and the inertia of the fluid

$$F = C_D A_p \rho_f U^2/2 . \qquad (2)$$

For a sphere $A_p = \pi d_p^2/4$ and we get

$$F = C_D \pi d_p^2 \rho_f U^2/8 . \qquad (3)$$

Then Eq. (*1*) can be expressed algebraically

$$\frac{\pi}{6} d_p^3 (\rho_s - \rho_f) g - C_D \frac{\pi}{8} d_p^2 \rho_f U^2 = \frac{\pi}{6} d_p^3 \rho_s \, dU/d\tau . \qquad (4)$$

When a particle attains its constant, free-fall or terminal velocity the accelerating force is zero, $(dU/d\tau) = 0$, and the weight of the particle is exactly balanced by the sum of the buoyancy and the resisting force caused by the flow of fluid around the particle. At such a steady state the force balance given by Eq. (*4*) can be recast into the dimensionless form as

$$C_D Re_t^2 = 4Ar/3 , \tag{5}$$

where

$$Re_t = U_t d_p \rho_f/\mu_f \tag{6}$$

is the Reynolds number and

$$Ar = d_p^3 \rho_f (\rho_s - \rho_f) g/\mu_f^2 \tag{7}$$

is the Archimedes number.

2.2. *Laminar Flow, Stokes Region* ($Re_t < 0.1$)

The simplicity of Eqs (*2*), (*3*) and (*5*) is, in practice, only illusive. In general, the drag coefficient C_D is a complex function of the flow conditions, i.e. $C_D = C_D(Re)$.

Under viscous or laminar (streamline, creeping) flow conditions ($Re_t < 0.1$) Stokes[3] demonstrated mathematically for settling spherical particles that the force opposing motion through a fluid is proportional to the viscosity of the fluid and is given as

$$F = 3\pi \mu_f d_p U_t , \qquad \text{the Stokes law,} \qquad Re_t < 0.1 . \tag{8}$$

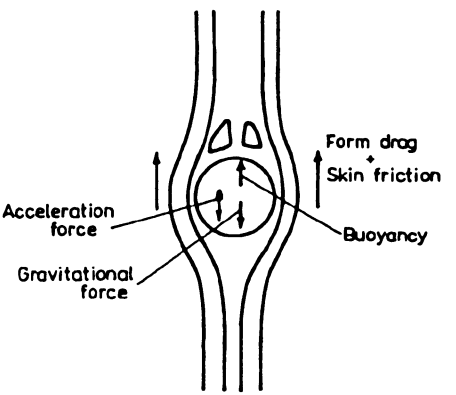

FIG. 1
Forces acting on a rigid, spherical particle falling through an infinite, homogeneous fluid

The steady state force balance, $(dU/d\tau) = 0$, on the particle in the Stokesian region then leads to

$$U_t = d_p^2 (\rho_s - \rho_f) g/18 \mu_f , \qquad Re_t < 0.1 \tag{9}$$

or

$$Re_t = Ar/18 , \qquad Re_t < 0.1 . \tag{10}$$

Combining Eqs (*3*) and (*8*) provides for the drag coefficient

$$C_D = 24/Re_t , \qquad Re_t < 0.1 , \tag{11}$$

which is analogous to the expression for the friction factor for laminar flow in smooth pipes (16/*Re*).

It should be noted that the Stokes law given by Eq. (*8*) is an analytical solution of the equation of motion and the continuity equation for $Re_t < 0.1$. No theoretical predictions of the drag coefficient can be made at higher values of the Reynolds number[3]. The dependence of the drag coefficient on the Reynolds number for $Re_t > 0.1$ is, therefore, deduced from experimental measurements.

In free fall particles with terminal Reynolds number $Re_t < 0.1$ attain their terminal velocity within fractions of a second. On the other hand, the time and distance taken to reach the terminal velocity become considerable for larger particles. The procedures for calculating the acceleration time and distance are reported by Heywood[4].

In experimental work, settling columns have to be large enough also in cross section to eliminate or minimize wall effects. This is of particular importance in the highly turbulent region where larger particles including spheres deviate considerably from a vertical path. For example Pettyjohn and Christiansen[5] employed a 0.5 m square settling column for the experimental measurements in turbulent flow and a 12.5 cm i.d. column for viscous or laminar flow experiments.

2. 3. *Turbulent Flow, Newton Region* ($1\,000 < Re_t < 2 . 10^5$)

In this flow region, the resistance force acting on a sphere is approximately proportional to the squared velocity of fluid flowing around the sphere. No satisfactory theoretical expressions for the drag force have been developed and the frictional loss has to be found by experiment.

A single value of the drag coefficient is often given as a first approximation in turbulent flow:

$$C_D \approx 0.44 , \qquad 1\,000 < Re_t < 2 . 10^5 . \tag{12}$$

As can be seen in Fig. 2 the drag coefficient is not actually constant in the Newton region. The dependence $C_D = C_D(Re_t)$ exhibits a feeble minimum of about 0.385 between Re_t = 2 000 and 5 000. The curve in Fig. 2 represents a large volume of experimental findings on the flow around a sphere. In this system, there is no clear transition from laminar to turbulent flow as it is for fluid flow in a tube. The discharge of vorticity increases in rate and irregularity with increasing Reynolds number, and eventually the wake becomes a completely turbulent mass of eddies and vortices.

The shape of the curve $\log C_D$ versus $\log Re_t$ is well established, based on numerous experimental data. The slope of the curve gradually changes from −1 to zero as the Reynolds number increases from about 10^{-2} to $2 \cdot 10^5$. At $Re \approx 2 - 3 \cdot 10^5$ turbulence develops to the rear of the sphere and the value of the drag coefficient falls to about 0.1 – 0.2.

Inserting Eq. (*12*) into Eq. (*5*) we get after rearrangement an approximate expression

$$U_t \cong \left(\frac{4}{3} \frac{d_p (\rho_s - \rho_f) g}{0.44 \rho_f}\right)^{1/2}, \qquad 1\,000 < Re_t < 2 \cdot 10^5. \qquad (13)$$

As indicated by this equation the terminal velocity is much less dependent on particle size than in the laminar regime (see Eq. (*9*)). The viscosity of fluid does not occur in the equation for U_t at all.

2. 4. *Transitional Flow, Transition Region* ($0.1 < Re_t < 1\,000$)

In most practical situations and applications of fluidized beds the particles of interest have their terminal velocities within the transitional regime and an accurate as well as rapid method of prediction is needed.

As mentioned above numerous attempts have mostly failed at developing theoretically based expressions to relate the drag coefficient with the Reynolds number.

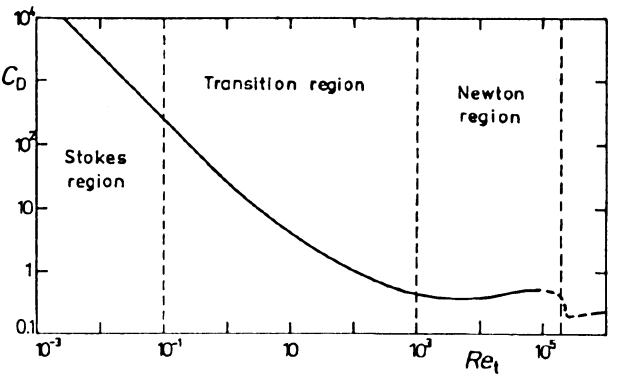

Fig. 2
Standard drag coefficient of spheres as a function of the Reynolds number

Considerable attention has been paid, therefore, to the experimental determination of the terminal velocity and drag coefficient for free-settling spherical particles. With the use of measured data on the free-fall of spherical particles in a broad spectrum of fluids, the drag coefficient is plotted as a function of the Reynolds number in Fig. 2. As shown in this figure the so-called standard drag curve has three broad regions corresponding to the different flow regimes as mentioned above. A sharp decrease of the curve at $Re \approx 2 \cdot 10^5$ is linked to a state when the boundary layer breaks off.

In essence, what is presented below are the results of efforts to find a mathematical approximation to experimental data collected on the drag coefficient of spheres. A number of empirical relationships are reported in the literature. A reader should always be careful about the range of their applicability.

Since the drag coefficient C_D is usually a non-trivial function of the Reynolds number which includes the terminal velocity, its estimation mostly depends on successive approximations. In order to eliminate the need of possibly tedious iterations, a convenient, but hardly accurate procedure was used in the past[2]. This method is based on the fact that the right hand sides of the dimensionless equations (*14*) and (*15*)

$$C_D Re_t^2 = \frac{4}{3} \frac{d_p^3 \rho_f (\rho_s - \rho_f) g}{\mu_f^2} \tag{14}$$

$$\frac{C_D}{Re_t} = \frac{4}{3} \frac{(\rho_s - \rho_f)}{\rho_f^2} \frac{\mu_f g}{U_t^3} \tag{15}$$

do not include the terminal velocity and the particle size, respectively. To find the terminal velocity of a given particle or the particle size corresponding to a certain terminal velocity, the calculated plots of $C_D Re_t^2$ or C_D/Re_t versus Re_t shown in Fig. 3 are employed.

In some cases it may be convenient but less accurate, to work with simplified expressions for C_D at medium and higher Reynolds numbers. In the transition region the drag coefficient can be very roughly approximated[3] as

$$C_D \approx 18.5/Re_t^{0.6} \qquad 2 < Re_t < 5 \cdot 10^2 . \tag{16}$$

Among well-known, and commonly employed expressions, for example in fluidized bed modelling, there is the semiempirical equation of Schiller and Neumann[6] which is valid over the range $0.1 < Re_t < 500 - 1\,000$.

$$C_D = 24 (1 + 0.15 Re_t^{0.687})/Re_t , \qquad 0.1 < Re_t < 500 - 1\,000 . \tag{17}$$

Khan and Richardson[7] have comprehensively reviewed the various empirical relations proposed for C_D by a number of workers in the field. They represent the available experimental data over only restricted ranges of the Reynolds number.

In some situations, the effects of the walls of the column and of neighbouring particles have to be taken into account[8]. Goldburg and Florsheim[9] observed fluctuations in the speed as well as in the direction of falling particles. They suggested that zig-zag or spiral paths of particles were associated with the onset of free stream turbulence.

3. PREDICTING TERMINAL VELOCITIES

3. 1. *Predictive Implicit Relationships for* U_t

The drag coefficient, C_D, in Eq. (5) is a complex function of the Reynolds number, Re_t, and then an iterative solution of Eq. (5) together with an expression for $C_D = C_D(Re_t)$ must be sought. Elementary technique such as interval halving has proven to be effective.

Some years ago Clift et al.[10] developed an empirical correlation for $C_D = C_D(Re_t)$ which is based upon a critical review of published experimental data. This correlation consists of a number of polynomial equations with a large number of fitted constants. Clift et al.[10] believe that this set of segment correlations presented in Table I is the best approximation to the standard drag coefficient for spheres at $Re_t < 10^6$.

The need for such a complicated, multisegment regression equation was questioned by Flemmer and Banks[11] and by Turton and Levenspiel[12]. The authors also proposed empirical, but very much simpler correlations for the drag coefficient of the freely falling spheres containing several fitted parameters. These relationships have also been

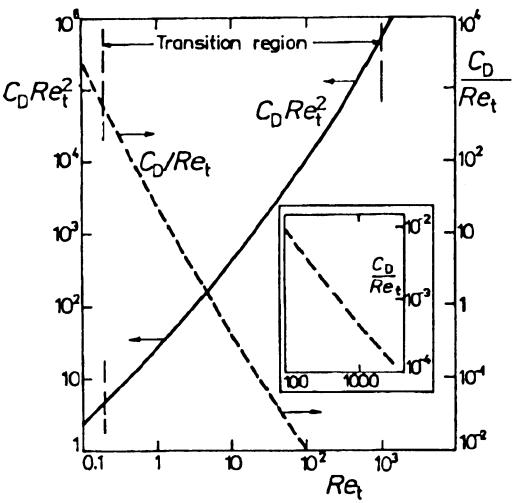

FIG. 3
Dimensionless groups $C_D Re_t^2$ and C_D/Re_t plotted as functions of the Reynolds number[2]

deduced from measured data and are given below. Flemmer and Banks[11] have put forward an equation of exponential form with five fitted parameters

$$C_D = 24 \cdot 10^{E}/Re_t , \qquad (18)$$

where

$$E = 0.261\, Re_t^{0.369} - 0.105\, Re_t^{0.431} - 0.124/[1 + (\log_{10} Re_t)^2] , \qquad (19)$$

$$Re_t < 3 \cdot 10^5 .$$

Turton and Levenspiel[12] have presented a correlation which has the form of a single equation also with fitted parameters

$$C_D = 24\,(1 + 0.173\, Re_t^{0.657})/Re_t + 0.413/(1 + 16\,300\, Re_t^{-1.09}) , \qquad (20)$$

$$Re_t < 2 \cdot 10^5 .$$

As can be seen the first term on the right hand side of Eq. (*20*) is very similar to the semiempirical expression of Schiller and Neumann[6] given by Eq. (*17*). Substituting Eq. (*20*) in Eq. (*5*) and rearranging gives Eq. (*21*)

$$Re_t^{3.09} + 10.053\, Re_t^{2.747} + 58.111\, Re_t^{2.09} + 163\,868\, Re_t^{1.657} -$$

$$- 3.22841\, Ar\, Re_t^{1.09} + 947\,215\, Re_t - 52\,623.1\, Ar = 0 . \qquad (21)$$

TABLE I
Drag coefficient correlations for the spheres proposed by Clift and Grace[10]

Correlation[a]	Range of applicability
$C_D = 3/16 + 24/Re$	$Re \le 0.01$
$\log_{10}[(C_D Re/24) - 1] = -0.881 + 0.82w - 0.05\, w^2$	$0.01 < Re \le 20$
i.e. $C_D = 24\,[1 + 0.1315\, Re^{(0.82 - 0.05\, w)}]/Re$	
$\log_{10}[(C_D Re/24) - 1] = -0.7133 + 0.6305\, w$	$20 < Re \le 260$
i.e. $C_D = 24\,(1 + 0.1935\, Re^{0.6305})/Re$	
$\log_{10} C_D = 1.6435 - 1.1242\, w + 0.1558\, w^2$	$260 < Re \le 1.5 \cdot 10^3$
$\log_{10} C_D = -2.4571 + 2.5558\, w - 0.9295\, w^2 + 0.1049\, w^3$	$1.5 \cdot 10^3 < Re \le 1.2 \cdot 10^4$
$\log_{10} C_D = -1.9181 + 0.6370\, w - 0.0636\, w^2$	$1.2 \cdot 10^4 < Re \le 4.4 \cdot 10^4$
$\log_{10} C_D = -4.3390 + 1.5809\, w - 0.1546\, w^2$	$4.4 \cdot 10^4 < Re \le 3.38 \cdot 10^5$

[a] $w = \log_{10} Re$.

The form of the polynomial Eq. (*21*) suggests a complicated behaviour of the function $Re_t = Re_t(Ar)$.

All the authors[10 - 12] claim that their own expression for the drag coefficient is the best correlation for the available data in the subcritical regime ($Re_t < 2 . 10^5$). In order to compare these equations, we have made systematic computations of the drag coefficient, C_D, for the Reynolds numbers ranging from 1 to 10^5 with the aid of these three correlations. The relative differences between the individual predictions and their mean values are presented in Fig. 4. As can be seen, the differences in C_D are practically always less than 4%, and these three correlations are equivalent from the standpoint of accuracy. The corresponding relative differences in the Reynolds number can be estimated from the expression

$$\frac{\Delta Re_t}{Re_t} = \frac{1 - (1 + \Delta C_D/C_D)^{1/2}}{(1 + \Delta C_D/C_D)^{1/2}} \qquad (22)$$

that has been deduced from Eq. (*5*). A deviation of 4% in C_D leads to an error of less than 2% in Re_t. All the three correlations exhibit a flat minimum ($C_D = 0.388 - 0.393$) in the range of the Reynolds numbers between 3 000 and 5 000. It can be stated that all the expressions provide accurate description of C_D over the entire practical range of the Reynolds number, i.e. for $Re_t < 2 . 10^5$.

Using the Turton and Levenspiel correlation (*20*) we have made systematic predictions of the free-fall conditions from Eq. (*21*) for selected values of the Archimedes number in the range between $Ar = 1$ and $4 . 10^7$. The estimated values of the Reynolds number, Re_t, as well as those of drag coefficient, C_D, are given in Table II. It

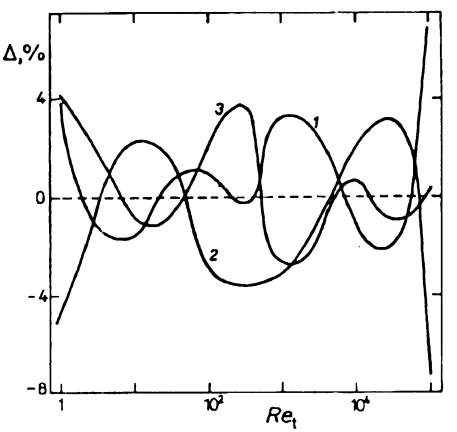

FIG. 4
Relative deviations of the drag coefficients of spheres Δ predicted by different correlations from their mean value. *1* Clift and Grace[10]; *2* Flemmer and Banks[11]; *3* Turton and Levenspiel[12]

is believed that these results are reliable representation of the free-fall conditions of spherical particles.

3. 2. *Predictive Explicit Expressions for* U_t

With the advent of personal computers there is no serious obstacle that solution of the equations needed must be sought using a numerical technique. Nevertheless, attempts have been made to develop explicit formulae that would make it possible to circumvent the iterative solutions of Eq. (5) together with an expression for the drag coefficient as a function of the Reynolds number.

Zigrang and Sylvester[13] proposed an explicit equation for particle settling velocities in liquid–solid systems in the form of the quadratic

TABLE II
Free-fall conditions predicted for spheres with the use of the Turton–Levenspiel correlation[12] for the drag coefficient

Ar	Re_t	C_D	Ar	Re_t	C_D	Ar	Re_t	C_D
1	0.054178	454.25	$5 . 10^2$	14.023	3.3902	$9 . 10^4$	454.52	0.58086
2	0.10686	233.53	$6 . 10^2$	16.078	3.0948	$1 . 10^5$	484.60	0.56777
3	0.15849	159.24	$7 . 10^2$	18.028	2.8717	$2 . 10^5$	733.40	0.49578
4	0.20927	121.78	$8 . 10^2$	19.891	2.6960	$3 . 10^5$	928.93	0.46355
5	0.25930	99.153	$9 . 10^2$	21.680	2.5531	$4 . 10^5$	1 095.2	0.44464
6	0.30864	83.982	$1 . 10^3$	23.404	2.4342	$5 . 10^5$	1 242.2	0.43204
7	0.35743	73.056	$2 . 10^3$	38.312	1.8168	$6 . 10^5$	1 375.1	0.42308
8	0.40569	64.810	$3 . 10^3$	50.720	1.5549	$7 . 10^5$	1 497.1	0.41642
9	0.45335	58.387	$4 . 10^3$	61.701	1.4009	$8 . 10^5$	1 610.5	0.41125
10	0.50059	53.208	$5 . 10^3$	71.716	1.2962	$9 . 10^5$	1 716.8	0.40714
20	0.95173	29.440	$6 . 10^3$	81.013	1.2189	$1 . 10^6$	1 817.0	0.40386
30	1.3738	21.194	$7 . 10^3$	89.750	1.1587	$2 . 10^6$	2 615.1	0.38993
40	1.7747	16.934	$8 . 10^3$	98.030	1.1100	$3 . 10^6$	3 213.6	0.38733
50	2.1586	14.308	$9 . 10^3$	105.93	1.0694	$4 . 10^6$	3 709.7	0.38754
60	2.5287	12.511	$1 . 10^4$	113.50	1.0350	$5 . 10^6$	4 141.1	0.38876
70	2.8867	11.200	$2 . 10^4$	177.69	0.84458	$6 . 10^6$	4 527.2	0.39033
80	3.2344	10.196	$3 . 10^4$	229.91	0.75674	$7 . 10^6$	4 879.3	0.39203
90	3.5730	9.3997	$4 . 10^4$	275.49	0.70273	$8 . 10^6$	5 204.8	0.39375
$1 . 10^2$	3.9033	8.7513	$5 . 10^4$	316.61	0.66506	$9 . 10^6$	5 508.6	0.39546
$2 . 10^2$	6.8824	5.6297	$6 . 10^4$	354.47	0.63669	$1 . 10^7$	5 794.5	0.39711
$3 . 10^2$	9.4788	4.4520	$7 . 10^4$	389.77	0.61436	$2 . 10^7$	8 062.9	0.41019
$4 . 10^2$	11.836	3.8071	$8 . 10^4$	423.01	0.59611	$4 . 10^7$	11 199	0.42525

$$U_t^2 - (2a + b^2) U_t + a^2 = 0, \tag{23}$$

where the coefficients a and b are given as

$$a = 1.8329 \left(\frac{(\rho_s - \rho_f) g d_p}{\rho_f} \right)^{1/2}, \tag{24}$$

$$b = 7.6190 \left(\frac{\mu_f}{\rho_f d_p} \right)^{1/2}. \tag{25}$$

Equations (23) – (25) are based upon the work of Barnea and Mizrahi[14] and that of Barnea and Mednick[15] on sedimentation and fluidization in liquid–solid systems. This general correlation was originally proposed to compute the settling velocity of the interface that develops during gravity sedimentation of monodisperse particles in different liquids. In its limit when the volume fraction of solids is equal to zero, the above expressions give the terminal velocity of an isolated spherical particle. With some effort the original equation of Zigrang and Sylvester can be rewritten into the dimensionless form as

$$Re_t = 1.8329 Ar^{1/2} + 29.025 - (106.4 Ar^{1/2} + 842.44)^{1/2}. \tag{26}$$

Having introduced the dimensionless diameter of the sphere defined by Eq. (27)

$$d^* = \left(\frac{3}{4} C_D Re_t^2 \right)^{1/3} = d_p \left(\frac{g \rho_f (\rho_s - \rho_f)}{\mu_f^2} \right)^{1/3} \tag{27}$$

and the dimensionless terminal velocity defined by Eq. (28)

$$U_t^* = \left(\frac{4}{3} \frac{Re_t}{C_D} \right)^{1/3} = U_t \left(\frac{\rho_f^2}{g \mu_f (\rho_s - \rho_f)} \right)^{1/3}. \tag{28}$$

Turton and Clark[16] have proposed an empirical correlation of another form

$$U_t^* = \left(\frac{1}{\left(\frac{18}{d^{*2}} \right)^{0.824} + \left(\frac{0.321}{d^*} \right)^{0.412}} \right)^{1.214}. \tag{29}$$

Equation (*29*) represents a weighed combination of the asymptotic relationships for very low and very high Reynolds numbers that is capable of describing the complete range of data in the subcritical region. With the use of the Reynolds and Archimedes numbers as variables

$$U_t^* = Re_t/Ar^{1/3} \tag{30}$$

$$d^* = Ar^{1/3} \tag{31}$$

the Turton and Clark equation can be recast into the form

$$Re_t = Ar^{1/3}/[(10.82/Ar^{0.549} + 0.6262/Ar^{0.137})^{1.214}], \quad Re_t < 2 \,.\, 10^5 . \tag{32}$$

Wesselingh[17] has put forward a similar interpolation formula which also covers the entire region of the flow conditions and can be rewritten in terms of Re_t and Ar as

$$Re_t = Ar^{1/3}/[(13.48/Ar^{0.6} + 0.6074/Ar^{0.15})^{1.111}], \quad Re_t < 2 \,.\, 10^5 . \tag{33}$$

In a recent work of ours[18,19], we have developed a polynomial equation for the free-fall conditions of a single particle

$$\log_{10} Re_t = P(A) + \log_{10} R(A), \qquad Ar < 10^8, \tag{34}$$

where

$$P(A) = [(0.0017795A - 0.0573)A + 1.0315]A - 1.26222 \tag{34a}$$

$$R(A) = 0.99947 + 0.01853 \sin (1.848A - 3.14) \tag{34b}$$

and

$$A = \log_{10} Ar . \tag{34c}$$

Accurate solutions of the polynomial equation (*21*) given in Table II have been employed in the least-squares fir that leads to Eq. (*34*).

The comparison of the measured terminal velocities of the glass spheres falling in dimethyl phthalate[18] and given in Table III with the estimates according to Eqs (*26*), (*32*) and (*34*) is shown in Fig. 5. It is apparent from Fig. 5 that the correlation of

Zigrang and Sylvester underpredicts somewhat the terminal velocity. The relative differences change from 4.2 to 6.2%. The corresponding relative deviations of the equation of Turton and Clark vary from +3.2% at Ar = 141 to −5.2% at Ar = 5 720. The proposed relationship (*34*) fits to the experimental data points with an excellent accuracy of +1.7 to −1.3%.

Very good agreement between the measured terminal velocities and the predictions of Eq. (*34*) has also been reported by Hirata and Bulos[20] for other liquid–solid systems. Nebrensky[21] has recently proposed a slightly different form of Eq. (*34*).

The explicit expressions for the terminal velocity (*26*), (*32*), (*33*) and (*34*) can also be viewed as more or less modified forms of a compilation of experimental data on the drag coefficient of spheres. In order to compare the explicit predictive equations, the values of the drag coefficient have been computed from the respective correlations with

TABLE III
Measured terminal velocities of the glass spheres falling in dimethyl phthalate[18] and the predictions of explicit Eq. (*34*). Properties of dimethyl phthalate at 25 °C: density, ρ_f = 1 189 kg m^{-3}; viscosity, μ_f = 13.23 mPa s

Solids	A	B	C	D	E	F
d_p, mm	1.119	1.201	2.046	2.504	3.220	4.080
ρ_s, kg m^{-3}	2 703.7	2 703.7	2 532.3	2 589.8	2 529.6	2 453.5
Ar	141.42	174.75	766.71	1 464.3	2 981.7	5 720.0
U_t exp., m s^{-1}	0.0516	0.0564	0.1046	0.1357	0.1738	0.2134
Re_t exp.	5.189	6.088	19.234	30.538	50.295	78.249
U_t calc., m s^{-1}	0.0507	0.0562	0.1035	0.1359	0.1751	0.2163

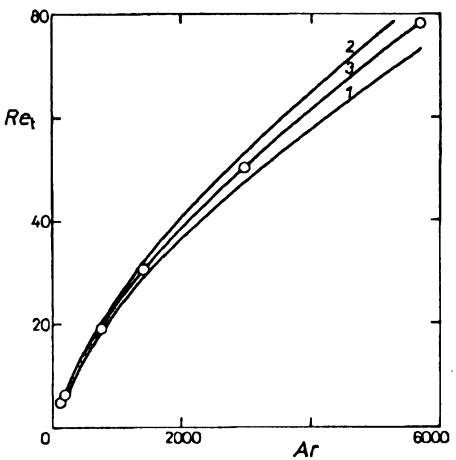

FIG. 5
Comparison of the terminal velocities at t = 25 °C measured on the glass spheres – dimethyl phthalate system with the predictions of the explicit relationships: ○ experimental data points[18]; *1* Zigrang and Sylvester[13]; *2* Turton and Clark[16]; *3* Hartman et al.[18,19]

the aid of Eq. (5). Such estimates have been compared with the values of the drag coefficient calculated with the use of the accurate solutions presented in Table II. The relative deviations of the respective predictions of Eqs (*26*), (*32*), (*33*) and (*34*) are plotted as functions of the Archimedes number in Fig. 6.

The equation by Zigrang and Sylvester[13] shows a systematic error and the largest deviations. With respect to the primary purpose of the original correlation, to predict the settling velocity of solid–liquid suspensions, this lower accuracy seems to be quite understandable. Both equations by Turton and Clark[16] and by Wesselingh[17] show a very similar behaviour. Their mean relative deviations amount to 11 and 10%, respectively. The maximum differences do not exceed –22 and –20%, respectively. As can be seen in Fig. 6, explicit relationship (*34*) provides an accurate description of the drag coefficient over a broad range of Archimedes number (i.e., $Ar < 4 \cdot 10^7$). The average deviation amounts to ± 2.6% and the maximum deviation is 6.2%. The corresponding relative differences in Reynolds number can be estimated with the aid of Eq. (*22*). The maximum deviations of Eq. (*32*) (–22%), Eq. (*33*) (–20%) and Eq. (*34*) (6.2%) in the drag coefficient lead to maximum errors of less than 13%, 12% and –3%, respectively, in the terminal Reynolds number. Although Eq. (*34*) may appear somewhat lengthy, its form is very convenient even for plain pocket calculators.

Having tried several forms of correlating equation, Khan and Richardson[7] have found as satisfactory representation of the available experimental results the following simple explicit expressions

$$C_D = (2.25\, Re_t^{-0.31} + 0.36\, Re_t^{0.06})^{3.45} \qquad (35)$$

$$Re_t = (2.33\, Ar^{0.018} - 1.53\, Ar^{-0.016})^{13.3} \qquad (36)$$

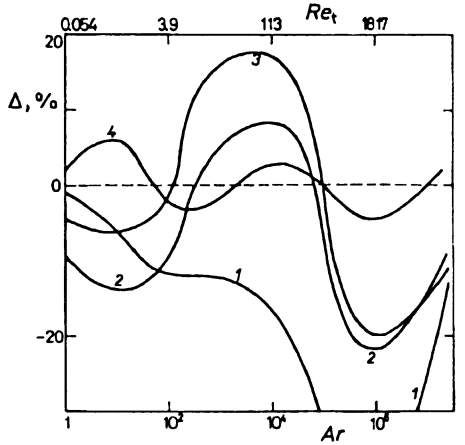

Fig. 6

Relative deviations of the drag coefficient Δ estimated from the explicit relationship for the particle terminal velocity: *1* Zigrang and Sylvester[13]; *2* Turton and Clark[16]; *3* Wesselingh[17]; *4* Hartman et al.[18,19]

$$Ar = (2.07\,Re_t^{0.27} + 0.33\,Re_t^{0.64})^{3.45} \qquad (37)$$

$$\text{for } 10^{-2} < Re_t < 3 \,.\, 10^5 \,.$$

Al-Salim and Geldart[22] have suggested an empirical relationship between Re_t and Ar that is valid over the range $0.1 < Re_t < 1\,000$. With respect to its length this expression is not given in the text.

4. INFLUENCE OF TEMPERATURE AND PRESSURE ON THE TERMINAL VELOCITY

Numerous industrial processes involve the units for contacting of gases with solids of widely different size. Such operations, usually accompanied by chemical reactions, are mostly carried out at elevated temperature and pressure.

An effect of temperature on the terminal velocity in the Stokes region (small particles) is indicated by Eq. (*9*)

$$U_t \sim \mu_g^{-1} \qquad Re_t < 0.1 \,. \qquad (38)$$

Since the viscosity of gas markedly increases with increase in temperature,

$$\mu_{\text{nitrogen}} = 1.5 \,.\, 10^{-6}\, T^{1.5}/(123.6 + T) \qquad (39)$$

$$\mu_{\text{air}} = 1.81 \,.\, 10^{-5}\, (T/293)^{0.66} \qquad (40)$$

the terminal velocity decreases with increasing temperature in laminar flow

$$U_t \sim T^{-0.6} - T^{-1}, \qquad Re_t < 0.1 \,. \qquad (41)$$

As suggested by Eq. (*13*) for the Newton region (large particles), the free-fall velocity is inversely proportional to the square root of the gas density

$$U_t \sim \rho_g^{-1/2}, \qquad 1\,000 < Re_t < 2 \,.\, 10^5 \,. \qquad (42)$$

The effect of temperature (and pressure) on the density of gas can usually be approximated from the equation of state of an ideal gas

$$\rho_g = 0.1203\,MP/T \qquad (43)$$

$$\rho_{\text{air}} = 3.489\,P/T \,. \qquad (44)$$

With respect to Eqs (*42*) – (*44*), it is apparent that

$$U_t \sim T^{1/2}, \qquad 1\,000 < Re_t < 2 \cdot 10^5. \tag{45}$$

In other words, increasing the temperature will cause an increase in the terminal velocities of particles falling in the Newton region.

In the transition region ($0.1 < Re < 1\,000$), the terminal velocity of particles falling in a gas is proportional to the power of the absolute temperature ranging between −1 and +0.5

$$U_t \sim T^{-1} - T^{0.5}. \tag{46}$$

This is the same range as in the case of the minimum fluidizing velocity. As follows from the definition, the relative change of the free-fall velocity with temperature is the sum of the partial changes in the Reynolds number, Re_t, gas viscosity and gas density. Relationship (*46*) indicates that the terminal velocity is a nonlinear function of temperature which can exhibit an extreme.

Some results of the systematic calculations in the transitional region for air are worth mentioning. There is approximately 35-fold decrease in the Archimedes number as the temperature increases from 0 to 1 000 °C. The terminal velocity of small particles ($d_p < 0.2$ mm, $\rho_s = 2\,500$ kg m^{-3}) monotonously decreases with the increasing temperature, i.e. $(dU_t/dT) < 0$. On the other hand, the free-fall velocity of larger particles ($d_p > 0.8$ mm, $\rho_s = 2\,500$ kg m^{-3}) monotonously increases as temperature is increased from 0 to 1 000 °C, i.e., $(dU_t/dT) > 0$.

Some of the results computed with the aid of Eqs (*34*), (*40*) and (*44*) are plotted in Fig. 7. As can be seen, the upper curve in this figure exhibits a distinct maximum at approximately 350 °C. When the particle size and/or particle density increase, the maximum on the curve $U_t = U_t(T)$ moves towards high temperatures. The compu-

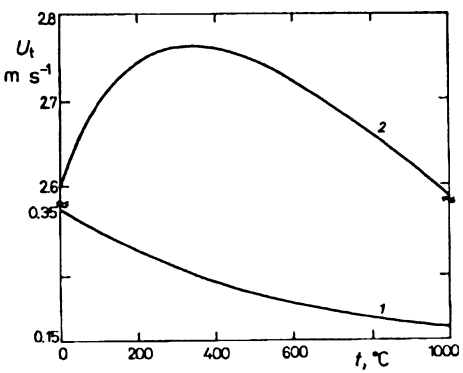

FIG. 7

Dependence of the terminal velocity on temperature for particles of different size predicted from Eq. (*34*): $\rho_s = 1\,500$ kg m^{-3}, medium: air. $d_p = 0.1$ mm (*1*), 0.5 mm (*2*)

tational results also show that the maximum occurs under the conditions expressed by $Re_t = 26 - 30$, i.e.,

$$dU_t/dT = 0; \qquad Re_t = 26 - 30 \tag{47}$$

$$U_t \sim T^0. \tag{48}$$

It is of interest to note that this value is not very far from that given for the minimum fluidization velocity[23]

$$dU_{mf}/dT = 0; \qquad Re_{mf} = 37 - 47. \tag{49}$$

The nonmonotonous behaviour of the functions $U_t = U_t(T)$ and $U_{mf} = U_{mf}(T)$ should be born in mind whenever the terminal velocity or the minimum fluidization velocity at operating conditions of interest are estimated from the values measured at ambient conditions.

Since $\rho_s >> \rho_g$ and the gas viscosity is practically independent of pressure, it can readily be seen from Eqs (*9*) and (*13*), how the terminal velocity will vary with pressure. The free-fall velocity is virtually independent of pressure in the Stokes region. As follows from Eq. (*13*), increasing the pressure can markedly reduce the terminal velocity in the Newton region.

$$U_t \sim P^{-1/2}, \qquad 1\,000 < Re_t < 2 \cdot 10^5. \tag{50}$$

5. NON-SPHERICAL PARTICLES

The resistance experienced by a particle moving in a fluid depends upon its shape and its orientation with respect to the direction of motion. The sphericity is usually employed as the single measure for characterizing the shape of non-spherical or irregular particles. It is introduced as the ratio

$$\psi = \text{surface of sphere / surface of particle} \tag{51}$$

at the same volume.

However, the sphericity is a theoretical concept which can only be realized imperfectly. There is no simple generally accepted method for measuring the sphericity of smaller irregular particles. The values given in Table IV should be regarded as approximate estimates only. Observing the particles of interest through a microscope and comparison with Table IV can enable a realistic value of the sphericity to be estimated. Another way to find the sphericity is to use the Ergun equation[24 - 26] for pressure drop across the fixed bed or the chart of Brownell et al.[27] for randomly packed beds

provided the porosity of the bed is known. Although the sphericity is undoubtedly a useful parameter, experience shows that particles with similar values of Ψ can have different shapes.

Another parameter important for nonisometric particles is the slimness (length to diameter) ratio. Solids of widely nonisometric shapes do not fall vertically at a constant velocity but can follow a zig-zag path or rotate. The free orientation of non-spherical particles moving by an unhindered fall is given in Table V.

TABLE IV
Sphericities of different bodies and particles

Particle	Sphericity, Ψ	Particle	Sphericity, Ψ
Sphere	1.0	Crushed particles	0.5 – 0.7
Cube	0.81	Pellets	0.7 – 0.8
Cylinder, $h = d$	0.87	Wheat	0.85
Cylinder, $h = 5\,d$	0.70	Corn	0.75
Sharp sand	0.65	Crushed limestone	0.55
Round sand	0.85 – 0.95	Limestone calcine	0.75
Crushed lignite	0.4	Flakes	0.2
Brown coal ash	0.53	Corundum	0.82
Crushed coal	0.65 – 0.75		

TABLE V
Free-fall orientation of nonisomeric particles[28]

Re_t	Wake	Orientation
0.1 – 0.5	Irrotational	All orienttions are stable when there are three or more perpendicular axes of symmetry
0.5 – 200	Fixed vortices	Stable in position of maximum drag
200 – 500	Periodic discharge of vorticity	Unpredictable. Disk and plates tend to wobble, while fuller bluff bodies tend to rotate
500 – $3 \cdot 10^3$	Increasing disorder	
$3 \cdot 10^3$ – $2 \cdot 10^5$	Fully turbulent	Rotation about axis of least
$2 \cdot 10^5$	Boundary layer becomes turbulent. Wakes of rounded bodies narrow	inertia, frequently coupled with spiral translation

In spite of apparent limitations, most predictive expressions employ the sphericity as a correction factor. For isometric or approximately isometric particles, Pettyjohn and Christiansen[5] introduced the corrections to the spherical particle equations as follows. For the Stokes region

$$U_t = K\,[d_p^2\,(\rho_s - \rho_f)\,g/18\,\mu_f]\,, \qquad Re_t < 0.1\,, \tag{52}$$

where

$$K = 0.843 \log_{10}(\Psi/0.065)\,, \qquad 0.67 < \Psi < 1\,. \tag{53}$$

Under turbulent flow conditions, Newton's modified equation can be employed

$$U_t = \left[\frac{4}{3}\,\frac{d_p\,(\rho_s - \rho_f)\,g}{C_R\,\rho_f}\right]^{1/2}, \qquad 2\,.\,10^3 < Re_t < 2\,.\,10^5\,, \tag{54}$$

where

$$C_R = 5.31 - 4.88\,\Psi\,, \qquad 0.67 < \Psi < 1\,. \tag{55}$$

For spherical particles ($\Psi = 1$), Eq. (53) provides $K = 1.0$ ($Re_t < 0.1$) and Eq. (55) gives $C_R = 0.43$ ($2\,.\,10^3 < Re_t < 2\,.\,10^5$).

Under flow conditions in the transition range, $0.1 < Re_t < 2\,000$, Pettyjohn and Christiansen[5] recommend that the curves $C_R = C_R(Re_t, \Psi)$ given in their study be used. However, simple interpolation seems to be more feasible and more accurate than repeated manipulations with the charts given in logarithmic scales. The terminal Reynolds number, $(Re_t)_{sph}$, and the terminal velocity, $(U_t)_{sph}$, are predicted for a sphere having the same d_p as a given isometric particle with the aid of e.g. Eq. (34). If the sphericity of the particle, Ψ, is not known, it can be approximately estimated from Table IV and the values of the coefficients K and C_R are calculated. It can easily be seen that

$$U_t/(U_t)_{sph} = K \qquad \text{at } Re_t = 0.1 \tag{56a}$$

and

$$U_t/(U_t)_{sph} = (0.43/C_R)^{1/2} \qquad \text{at } Re_t = 2\,000\,. \tag{56b}$$

The interpolation between these points provides the desired terminal velocity

$$U_t/(U_t)_{sph} = (0.43/C_R)^{1/2} + \\ + [K - (0.43/C_R)^{1/2}]\,[(2\,000 - (Re_t)_{sph})/(2\,000 - 0.1)] \tag{57}$$

$$\text{for } 0.1 < Re_t < 2\,000\,.$$

The extent to which the results of Pettyjohn and Christiansen[5] can be applied to nonisomeric particles is not clear.

Becker[28] undertook an experimental study that also included nonisometric particles. The correlations of the inertial drag coefficient proposed cover a broad spectrum of shapes and orientations. They extend over a full range of the Reynolds number.

For highly irregular shaped solids, the best that can be done is to determine the terminal velocity by experiment.

Alternatively, the curves in Fig. 8 can be employed for first approximations. These curves, presented in a monograph by Levenspiel[29] are based on data amassed by different investigators.

6. CONCLUSIONS

The terminal velocity of spherical particles falling in an infinite Newtonian fluid can accurately be predicted with the use of any of the empirical correlations given in Table I and by Eqs (*18*) and (*20*). These different expressions for the drag coefficient of the spheres are equivalent from the standpoint of their accuracy. The employment of the explicit Eq. (*34*) eliminates the need for iterative computations without a significant loss in accuracy.

Increasing the temperature brings about a decrease in the terminal velocity of smaller particles and an increase of the terminal velocity for larger particles. In general, the dependence $U_t = U_t(T)$ is not monotonous and exhibits a maximum at $Re_t = 26 - 30$ for the free-fall in air. An increase in pressure has very little effect for small particles and reduces the free-fall velocity of larger particles.

Some progress has also been made with nonspherical particles. It is believed that the realistic values of the terminal velocity of different isometric solids can be estimated.

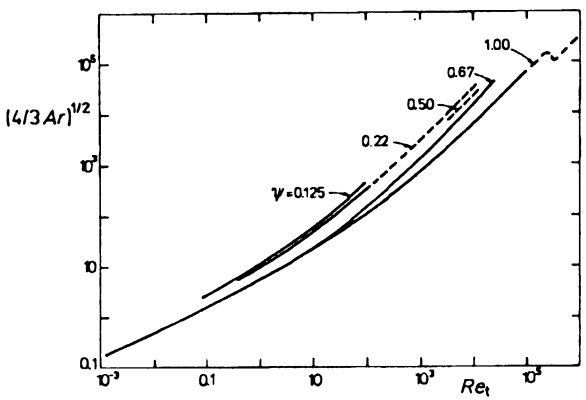

FIG. 8
Chart for estimation of the terminal velocity of nonspherical particles falling through fluids[29]

In the case of highly irregular and nonisometric particles, the free-fall velocity as well as the overall behaviour of such particles should be determined by experiment.

The author would like to acknowledge that his contribution to this paper was in part supported through Academy of Sciences of the Czech Republic, Grant No. 47208.

SYMBOLS

A	$= \log_{10} Ar$ in Eq. (34)
A_p	projected area of particle perpendicular to direction of motion, m^2
Ar	Archimedes number, $Ar = d_p^3 g \rho_f(\rho_s - \rho_f) / \mu_f^2$
a	coefficient defined by Eq. (24)
b	coefficient defined by Eq. (25)
C_D	drag coefficient of sphere
ΔC_D	inaccuracy in drag coefficient
C_R	coefficient of resistance defined by Eqs (54) and (55)
d_p	diameter of sphere, m
d^*	dimensionless diameter of sphere defined by Eq. (27)
F	force acting on particle
g	acceleration due to gravity, m s^{-2}
K	Stokes law shape factor defined by Eqs (52) and (53)
M	molecular weight, kg $kmol^{-1}$
P	pressure, kPa
Re_{mf}	Reynolds number at minimum fluidization, $Re_{mf} = U_{mf} d_p \rho_f/\mu_f$
Re_t	Reynolds number at terminal velocity of particle, $Re_t = U_t d_p \rho_f/\mu_f$
ΔRe_t	inaccuracy in Re_t
t	temperature, °C
T	temperature, K
U	superficial fluid velocity, m s^{-1}
U_{mf}	minimum fluidizing velocity, m s^{-1}
U_t	terminal, free-fall velocity of particle, m s^{-1}
w	$= \log_{10} Re$
Λ	relative deviation, %
μ_f	fluid viscosity, Pa s
ρ_f	fluid density, kg m^{-3}
ρ_g	gas density, kg m^{-3}
ρ_s	particle density, kg m^{-3}
τ	time, s
Ψ	particle sphericity, shape factor

Subscripts

calc	calculated
exp	experimental
sph	sphere

REFERENCES

1. Yates J. G.: *Fundamentals of Fluidized-Bed Chemical Processes*, p. 37. Butterworths, London 1983.
2. Geldart D. in: *Gas Fluidization Technology* (D. Geldart, Ed.), p. 123. Wiley, Chichester 1986.
3. Bird R. B., Stewart W. E., Lightfoot E. N.: Přenosové jevy, p. 207. Academia, Praha 1968.
4. Heywood H. in: *Proceedings of Symposium on Interaction between Fluids and Particles*, p. 1. Inst. Chem. Engrs., London 1962.
5. Pettyjohn E. S., Christiansen E. B.: Chem. Eng. Prog. *44*, 157 (1948).
6. Schiller L., Neumann A.: Z. Ver. Deut. Ing. *77*, 318 (1933).
7. Khan A. R., Richardson J. F.: Chem. Eng. Commun. *62*, 135 (1987).
8. Khan A. R., Richardson J. F.: Chem. Eng. Commun. *78*, 111 (1989).
9. Goldburg A., Florsheim B. H.: Phys. Fluids *9*, 45 (1966).
10. Clift R., Grace J. R.: *Bubbles, Drops and Particles*. Academia Press, New York 1978.
11. Flemmer R. L. C., Banks C. L.: Powder Technol. *48* 217 (1986).
12. Turton R., Levenspiel O.: Powder Technol. *47*, 83 (1986).
13. Zigrang D. J., Sylvester N. D.: AIChE J. *27*, 1043 (1981).
14. Barnea E., Mizrahi J.: Chem. Eng. J. *5*, 171 (1973).
15. Barnea E., Mednick R. L.: Trans. Inst. Chem. Eng. *53*, 278 (1975).
16. Turton R., Clark N. N.: Powder Technol. *53*, 127 (1987).
17. Wesselingh J. A.: Chem. Eng. Process. *21*, 9 (1987).
18. Hartman M., Havlín V., Trnka O., Čársky M.: Chem. Eng. Sci. *44*, 1743 (1989).
19. Hartman M., Veselý V., Svoboda K., Havlín K.: Collect. Czech. Chem. Commun. *55*, 403 (1990).
20. Hirata A., Bulos F. B.: J. Chem. Eng. Jpn. *23*, 599 (1990).
21. Nebrensky J. R.: Chem. Eng. Sci. *45*, 1653 (1990).
22. Al-Salim Q. A. W., Geldart D.: Powder Technol. *3*, 253 (1969/1970).
23. Hartman M., Svoboda K.: Ind. Eng. Chem., Process Des. Dev. *25*, 649 (1986).
24. Ergun S.: Chem. Eng. Prog. *48*, 89 (1952).
25. Pata J., Hartman M.: Ind. Eng. Chem., Process Des. Dev. *17*, 231 (1978).
26. Svoboda K., Hartman M.: Ind. Eng. Chem., Process Des. Dev. *20*, 319 (1981).
27. Brownell L. E., Dombrowski H. S., Dickey C. A.: Chem. Eng. Prog. *46*, 415 (1950).
28. Becker H. A.: Can. J. Chem. Eng. *37*, 85 (1959).
29. Levenspiel O.: *Engineering Flow and Heat Exchange*, p. 152. Plenum Press, New York 1984.

Translated by the author (M. H.).